Elucidating signals that guide elongation of the *Drosophila melanogaster* dorsal-appendage tubes

Lara Backman

A thesis

submitted in partial fulfillment of the

requirements for the degree of

Master of Science

University of Washington

2013

Committee:

Celeste Berg

Susan Parkhurst

Barbara Wakimoto

Program Authorized to Offer Degree:

Molecular and Cellular Biology Program

Introduction

The formation of tubes, also known as tubulogenesis, is an important process in animal development. Tubulogenesis is required to create organs such as the heart, lungs, kidneys, and the spinal cord and brain. The patterning of tubular structures is fairly well understood, as are the movements required to form tubes from epithelial sheets (Hogan and Kolodzej, 2002; Lubarsky and Krasnow, 2003). The process by which already formed tubes migrate and change shape to achieve their final morphology, however, is relatively understudied.

Tubulogenesis begins when a patch of cells is set aside and fated to become a tubular structure. Tube patterning occurs in many different ways, depending on the organism and the structure formed. In the chick, an FGF8 signal renders cells sensitive to the BMP antagonists that pattern them into the neural plate, which will eventually form the neural tube (Streit *et al.*, 2000). FGFs are also crucial in patterning the mouse lung buds (Groenmenn *et al.*, 2004). The patch of cells that will form the dorsal appendages on *Drosophila* egg chambers is formed by the interplay of Decapentaplegic (DPP), which defines anterior fate, and Gurken (GRK), conferring dorsal fate; these signals are orthologues of BMP and EGF signals (Peri and Roth, 2000). In addition, Notch helps refine the patch into two distinct cell populations; one will form the roof and sides of each tube and the other will form the floor of the tubes (Ward *et al.*, 2006). Subsequently, WNT signals may help sharpen the boundaries between these two cell populations (Jordan *et al.*, 2005).

Once cells are fated to become tubes, they must change shape and move to form tubes. In both mouse neural-tube formation and *Drosophila* dorsal-appendage formation,

the cells fated to become the tube thicken and form a placode (Dorman *et al*., 2004; Schoenwolf and Powers, 1987). The cells of the placode become wedge shaped by constricting apically or via other means, resulting in placode invagination. Placode formation, apical constriction, and subsequent invagination is fairly common and is used to form the vertebrate lung and liver, the *Drosophila* trachea and salivary glands, and other organs (Hogan and Kolodzej, 2002). In contrast, the zebrafish neural tube forms by making a cord of cells, which then hollows itself to form a lumen (Horne-Badovinac *et al.*, 2001).

The dorsal appendages (DAs) of the *Drosophila melanogaster* egg provide an excellent model system for studying tube guidance. The DAs are nonessential eggshell structures that facilitate gas exchange for the embryo (Fig. 1; Hinton, 1969). The DA tubes begin as two patches of anterior columnar follicle cells, one on each side of the dorsal midline. Each patch is composed of two distinct cell populations: the anterior and midline edge of the patch make up the floor cells, which will form the floor of the tube,

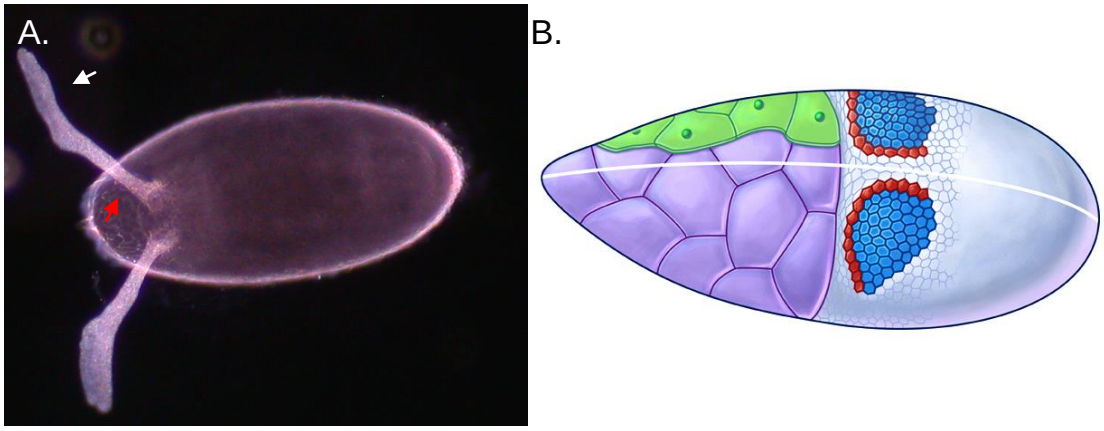

Figure 1. *Drosophila melanogaster* eggshell and schematic of DA patterning. A. Micrograph showing a dorsal view of a wild-type egg. Note the stalk (red arrow) and paddle (white arrow) shape of the dorsal appendages. B. Schematic of a stage-10B egg chamber. The stretch cells (green) overlie the nurse cells (purple), while the columnar cells, including the roof-forming cells (blue) and floor cells (red) overlie the oocyte. Part B taken from Dorman *et al.*, 2004.

while the remainder of the patch are the roof cells, which will form the roof and sides of the tube (Fig. 1, Dorman *et al*., 2004). During DA morphogenesis, the floor cells dive under the roof cells and zipper together to form a tight seal. Simultaneously, the apices of the roof cells constrict, causing the whole placode to bulge outward and curve, facilitating tube formation. During this process, lateral cells move toward the midline in a process known as convergence and extension (Ward and Berg, 2005; Davidson and Keller, 1999). During tube elongation, both roof and floor cells continue to intercalate, while roof cells then expand their apices while shortening their lateral edges. These behaviors extend the tube over the stretch cells (SCs). Finally, roof cells secrete chorion into the lumen, forming the DAs (Dorman *et al*., 2004).

It is during tube expansion where guidance comes into play. The tubes must assume the generally correct morphology at this stage, which begins at stage 12 and lasts until stage 13, although they may continue to refine the rough initial shape during stage 14 (Dorman *et al.*, 2004; Boyle and Berg, 2009). Several lines of evidence suggest the existence of a guidance signal for the dorsal-appendage tubes; the most convincing was obtained from studies of the *bullwinkle* mutant. In fact, genetic evidence demonstrated that multiple signaling events facilitate DA tubulogenesis. The SOX transcription factor encoded by *bullwinkle* (*bwk*) is required in the germline cells (Rittenhouse and Berg, 1995), yet causes a phenotype in the dorsal-appendage-forming cells, showing that there must be communication between the germline and dorsal-appendage-forming cells. Two non-receptor tyrosine kinases, SHARK and SRC42A, are required in the SCs to transduce this signal (Tran and Berg, 2003). The SCs must then communicate with the tube-forming cells. In *bwk* and *shark* mutants, the DAs branch and form prong-like structures

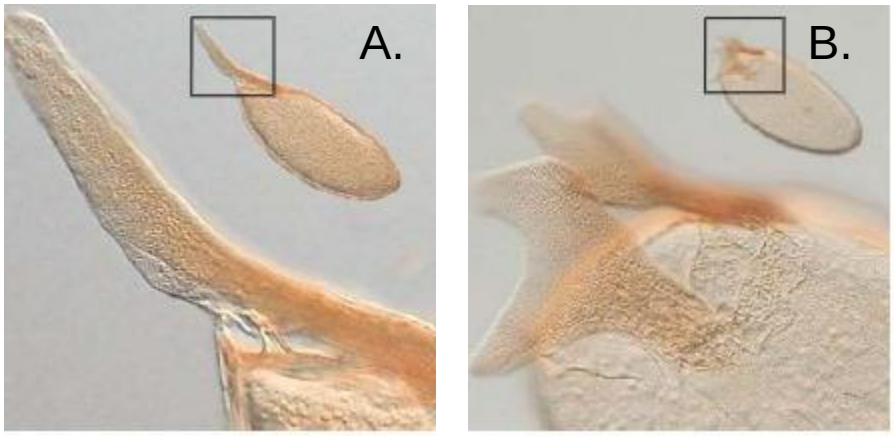

Figure 2. Dorsal appendages in wild-type and *bwk* eggs. Laid eggs. Each panel shows an entire egg in the top right corner (DA boxed) and a higher magnification view of the DAs. A. Wild-type egg with a long, slender stalk and narrow paddle. B. *bwk* egg; note the short, broad paddle that resembles a moose antler. Images from Dorman *et al.*, 2003.

(Fig. 2; Rittenhouse and Berg, 1995; Tran and Berg, 2003), revealing the defects in tube morphology when the DA tubes lack signals from the germ line and SCs. Additionally, the heterotrimeric G-protein subunits Gbeta13F and Galpha12 (encoded by *concertina* and its partial duplicate *CG40005*) are required in the DA-forming cells for correct DA formation (Boyle *et al*., 2010; Altaras, Abuan, and Berg, unpublished data). The nature of the signals and the exact mechanism of DA guidance are not yet known. A number of known developmental signals are good candidates for such a guidance signal; the most likely candidates from all the pathways are the Wnt, Hh, and axon-guidance pathways, as discussed below.

The WNT pathway is among the most promising as a candidate signaling pathway for SCs to communicate with the tube-forming cells. Wnts are secreted ligands that require lipidation by the Porcupine family of proteins prior to release from the cell (Proffitt and Virshup, 2012). They can act as short-range and long-range morphogens (Niehrs, 2012). The Wnts' canonical receptors are members of the Frizzled protein

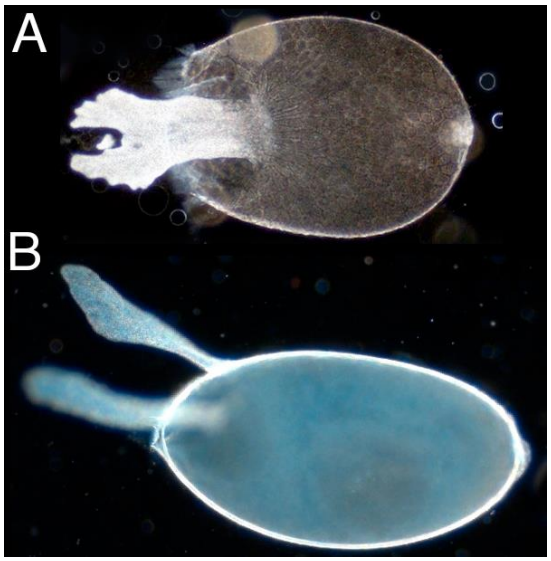

Figure 3. The *frizzled* DA defects. A. Egg laid by a female homozygous for a strong fz allele, *fz[H51]*. The fused DAs are due to patterning defects but the wavy paddles are due to morphogenesis defects. The short, round egg phenotype is consistent with a PCP defect. B. *fz*-RNAi expressed with *act5C-GAL4* throughout the follicular epithelium creates short DAs with enlarged paddles. Image A provided by David Strutt and B by Philip Louie.

family. Frizzled proteins are G-protein-coupled receptors (GPCRs), which might explain the necessity for G proteins in DA formation (Niehrs, 2012). Furthermore, a mutation in *frizzled* produces an odd branching dorsal-appendage phenotype, suggesting a role for Wnts in DA formation (Fig. 3; Louie and Berg, unpublished data; David Strutt, personal communication). Frizzleds are also involved in the planar cell polarity (PCP) pathway, although their ligand for this pathway in flies is unclear (Maung and Jenny, 2011; Fenstermaker *et al.*, 2010).

Another good candidate for a guidance signal is the Hedgehog protein. Hedgehog signaling also uses a GPCR, Smoothened (Kar *et al.*, 2012). Hedgehog binds to its receptor, Patched, which then causes the accumulation and high activity of Smoothened by an unknown mechanism. This interaction leads to a signal cascade that prevents the degradation of the transcription factor Cubitus interruptus, which then translocates to the nucleus and affects target gene expression (Kar *et al.*, 2012).

Axon-guidance molecules, such as the Netrins, Ephrin, and the Semaphorins, are also good candidates for a potential SC-to-DA signal. All three guidance molecules are

cell-surface-bound signals and can have either attractive or repulsive effects on nearby axon growth cones (Serafini *et al.*, 1994; Villar-Cerviño *et al.*, 2013; Tran *et al.*, 2007). These molecules are not only known for their roles in guiding axons, but also for a function in angiogenesis, both as potentially attractive and repulsive molecules (Neufield *et al.*, 2012; Castets and Mehlen, 2010; Salvucci and Tosato, 2012).

The experiments described in this thesis aimed to determine what, if any, signals are involved in the guidance of the DA tubes. To study signals important in tube guidance, I used a two-pronged approach. First, I added inhibitors and activators of candidate signaling pathways to egg chambers developing in an *in vitro* culture system to temporally control activity of signaling molecules and avoid interference with early patterning events. Secondly, I used an RNAi approach to knock down production of candidate signaling molecules in the SCs of the egg chamber, giving tight spatial control of signal interference. Preliminary data analyzing 5 signaling pathways suggest that the Wnt pathway may play a role in DA guidance mainly through Wnt2, although other Wnts may be involved in DA guidance.

Methods

Fly strains

See Table 1. VDRC is an abbreviation for the Vienna *Drosophila* Resource Center.

Egg chamber culture conditions

I fattened adult female flies of the w^{1118} or *E(spl)m7-lacZ* genotypes on wet yeast with males present and with daily transfer to fresh vials for a minimum of two days prior to dissection. I anesthetized the flies with CO_2 and dissected the females in room-

Table 1. Fly strains.

Common name	CG number	Genotype	Origin
w^{1118}	CG2759	*w*^{1118} ; + ; +	Rubin lab
PG150	N/A	y[*] w[*] P{GawB=w[+mW.hs]GAL4}l(1)3At[PG150] P{ry[+t7.2]=neoFRT}19A/FM6, B[1] dm[1] sc[8] y[31d] ; P{w[+mC]=UAS-GFP.nls}14 P{w[+mC}=tubP-GAL80[ts]}20/CyO ; +	Created by Faith Hassinger from a stock from the Edgar lab
UAS-GFP	N/A	w[*] ; + ; P{w[+mC]=UAS-GFP.S65T}T10	Bloomington 1522
NGoF	CG3936	y[*] w[*] ; P{w[+mC]=UAS-Dl::N.ΔECN}B2a2/CyO ; +	Ruohola-Baker lab
E(spl)m7-lacZ	N/A	w[*] ; + ; p{w[+*]=E(spl)m7-lacZ}	Deng lab
bunched-lacZ	CG5461	+ ; P{PZ=ry[+t7.2]PlacZ}bun[l(2)07692] cn[1]/CyO, cn[2] ; ry[506]	Spradling lab
Hh RNAi	CG4637	*w1118* ; + ; P{GD1933v1402 w+}	VDRC 1402
Hh RNAi	CG4637	*w1118* ; + ; P{GD6242v43255 w+}	VDRC 43255
Hh RNAi	CG4637	y[*] w1118; P{KK108916}VIE-260B ; +	VDRC 109454
Wg RNAi	CG4889	y[*] w1118; P{KK108857}VIE-260B ; +	VDRC 104579
Wnt2 RNAi	CG1916	y[*] w1118; P{KK107678}VIE-260B ; +	VDRC 104338
Wnt4 RNAi	CG4698	y[*] w1118; P{KK102348}VIE-260B ; +	VDRC 104671
Wnt5/3 RNAi	CG6407	y[*] w1118; P{KK105240}VIE-260B ; +	VDRC 101621
Wnt6 RNAi	CG4969	y[*] w1118; P{KK107855}VIE-260B ; +	VDRC 104020
Wnt10 RNAi	CG4971	y[*] *w1118* ; P{KK104943}VIE-260B ; +	VDRC 100867
WntD RNAi	CG8458	y[*] w1118; P{KK103987}VIE-260B ; +	VDRC 107727
Sema-1a RNAi	CG18405	y[*] w1118; P{KK109430}VIE-260B ; +	VDRC 104505
Sema-2b RNAi	CG33960	y[*] w1118; P{KK105872}VIE-260B ; +	VDRC 108030
Sema-2b RNAi	CG33960	y[*] w1118; P{KK109911}VIE-260B ; +	VDRC 101842
Ephrin RNAi	CG1862	y[*] w1118; P{KK102026}VIE-260B ; +	VDRC 105139
Netrin A RNAi	CG18657	y[*] w1118; P{KK101369}VIE-260B ; +	VDRC 108577
Opa1 RNAi	CG8479	w[*] ; P{w+[mC]=UASt-opa1-like-RNAi} ; +	VDRC 106290
CG9523 RNAi	CG9523	w[*] ; P{w+[mC]=UASt-CG9523-RNAi} ; +	VDRC 105634

temperature Robb's complete medium (Robb, 1969; see Appendix A for complete composition). Briefly, I made Robb's medium without the linoleic acid, filter-sterilized it, sterilely placed it in 10 mL aliquots, and stored it at 4° C. I warmed the medium to room temperature and added fresh linoleic acid in ethanol as described (Robb, 1969) before each dissection. I removed ovaries from the females in a glass dissection dish and

transferred them by forceps to another dish containing Robb's medium, where I gently dissected individual egg chambers to remove them from the ovariole sheath. I selected stage-10B egg chambers and transferred them by glass micropipette to a dish with fresh medium. After all females were dissected, I removed all non-stage-10B egg chambers from the dish, and transferred the remaining egg chambers by glass micropipette to a 24-well plate with 1 mL of Robb's medium per well. As appropriate to the experiment, I added JAG peptide (1 mM stock, AnaSpec), IWR-1 (10 mM stock in DMSO, Sigma), or DMSO (as a control) to the medium. I incubated the egg chambers overnight at 25° C and tallied their final stage of development.

Fixation of cultured egg chambers and preparation for imaging

After the culture period, I staged the egg chambers and gently disengaged them from the plastic well with forceps. I removed egg chambers into a 1.5-mL tube with a glass micropipette. I removed excess liquid by aspiration, and incubated the egg chambers in 400 µL of freshly prepared 4% formaldehyde in PBS for 30 minutes with nutation. I then washed them 3x in PBS for five minutes with nutation. Finally, I added 500 µL 50% glycerol in PBS and stored the tube at 4 °C until imaging.

Imaging

I placed egg chambers in 50% glycerol on a glass coverslip with a 200-µL micropipette set to 30 µL. I removed the excess glycerol with a P200 pipettor, and removed any remaining glycerol with a Kimwipe. I added 30 µL of 75% glycerol in PBS to the coverslip, which I then picked up with a glass slide. I performed dark-field imaging on a Nikon Microphot FXA microscope with a Nikon Coolpix digital camera. I took images with each appendage in focus; if both were in focus in a single shot, I took only one

image of that egg. I took most images with only one egg per frame, but sometimes multiple eggs could not be separated and were thus photographed together.

β-galatactosidase staining assay

To analyze expression of *lacZ* reporters *bunched-lacZ* and *E(spl)m7-lacZ*, I used a standard method developed for flies (Simon *et al.*, 1985).

RNAi crosses and conditions

I collected virgin female *w** *P{w*$^{+}$*, PG150-GAL4}/FM6, w, B[1] dm[1], sc[8], y[31d] ; P{w*$^{+}$*, gal80[ts]}/CyO; +/+* flies and aged them two days on wet yeast at 25° C. I then examined the females for morbidity and put 5 in each vial. I added 3 males of the listed

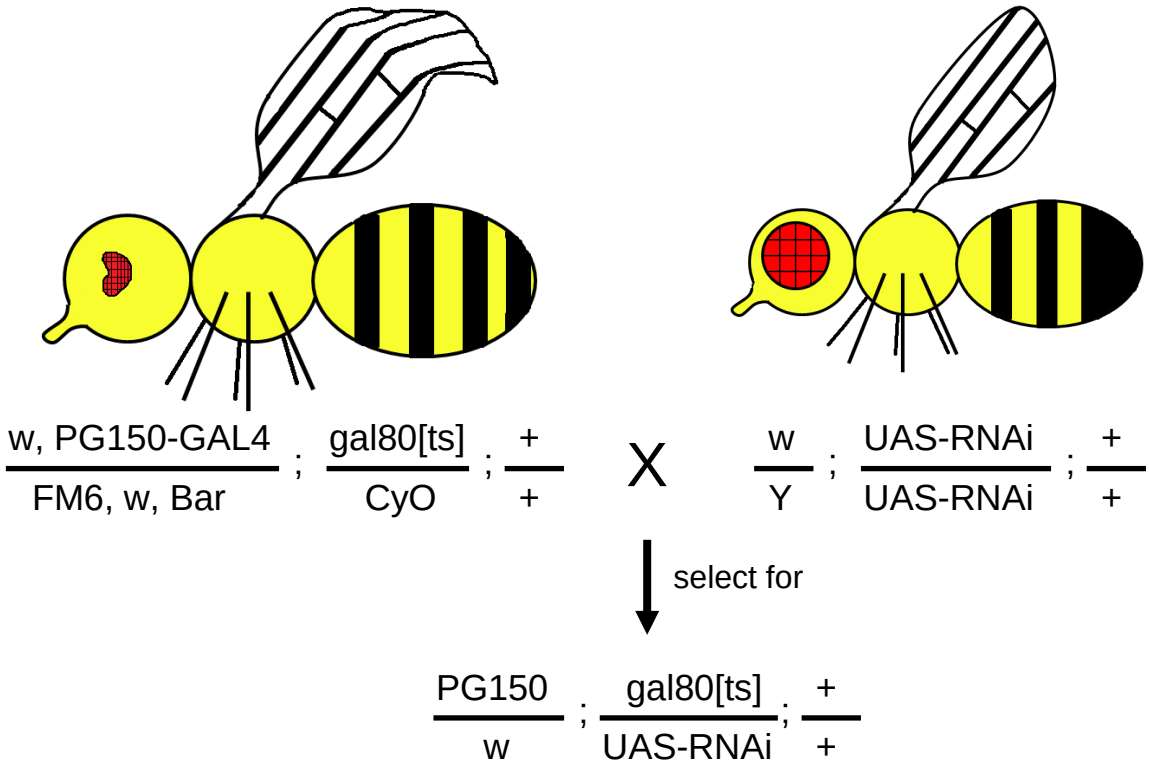

Figure 4. Mating scheme used to obtain RNAi expression in the ovary. I crossed virgin female *w P{w+, PG150-GAL4}/FM6, w, B[1] ; P{w+, gal80[ts]}/CyO; +/+* flies to males from each RNAi stock. The desired progeny represented 1/8 of the offspring.

genotype (Table 2, Table 3, Table 4) to these fresh vials, and allowed the flies to mate at 25° C for the first experiment and at 18° C for the second and third trials (Fig 4). I raised larvae at 25° C for the first experiment, 21° C for the second experiment, and at both 21° C and 25° C for the third experiment. When the progeny eclosed, I screened for the presence of the *PG150-GAL4* driver by choosing females with eyes that were non-Bar; that is, the eyes were round and displayed no notch. I also screened for the presence of the temperature-sensitive-*gal80* construct by selecting females without curly wings. I raised them at 30° C for 2 days on wet yeast with males. I placed a maximum of 20 females per cross with half their number in males in laying cages and kept them at 30° C, switching out laying plates every 8 hours. If fewer than 20 females of the correct genotype were available, I used all the available females. I collected eggs from the plates, stored them, and mounted them in Hoyer's solution as previously described (Wieschaus and Nüsslein-Volhard, 1986). I imaged the slides while blinded to genotype, and scored each appendage for severity of defect, with a "0" being no or very little defect, "1" being a slight defect, and "2" being a severe defect.

Measurement of DAs and statistical analysis

I measured appendages using the line tool in ImageJ, specifically measuring length from midpoint of base and maximum width of appendage (Fig. 5), and calculated their normalized width by dividing the maximum width by the length. I also categorized appendages as bifurcated, notched, or normal. I measured a subset of 20 appendages of each genotype from the initial set of RNAi experiments and used these data to determine the efficacy of each measurement for differentiating wild type from abnormal appendages. I measured six characters: 1) the length from base to tip, 2) the width

halfway up the appendage, 3) the maximum width, 4) the height from the base of the appendage to the maximum width, 5) the minimum width, and 6) the height from the base of the appendage to the minimum width (Fig. 5). Finally, I recorded the position of maximum and minimum widths and expressed each as a percentage of appendage length (0% at base, 100% at tip) for each chosen appendage. I analyzed the means using a one-way ANOVA with Gaines-Howell post-hoc test using the freely available PSPP software (http://www.gnu.org/software/pspp/). I analyzed categorical data with a chi-square test on VassarStats (http://www.vassarstats.net/csfit.html).

Results

Development of a quantitative assay for DA morphology

To quantify differences in DA morphology, it was necessary to have a set of parameters that define the shape of a mature dorsal appendage. To identify parameters to measure, I compared DAs of eggs laid by females produced by the first set of RNAi crosses. The "wild-type" flies were *bunched-lacZ, PG150-GAL4* not crossed to any RNAi line, and w^{1118}, while the "mutants" were 7 lines in which RNA interference was predicted to reduce the production of specific signaling components (see Table 2). I used a random-number generator to choose a subset of photographs from each genotype until I had measured twenty DAs of each genotype for my measurements. I then measured several parameters for each appendage: total length of appendage from midpoint of the base to the tip; width halfway along the appendage; maximum width; distance from base to the point of maximum width; minimum width; and distance from the base to the point of minimum width (Fig. 5). The length, maximum width, and minimum width evaluated the overall size of the appendage. The heights of the maximum and minimum widths, as

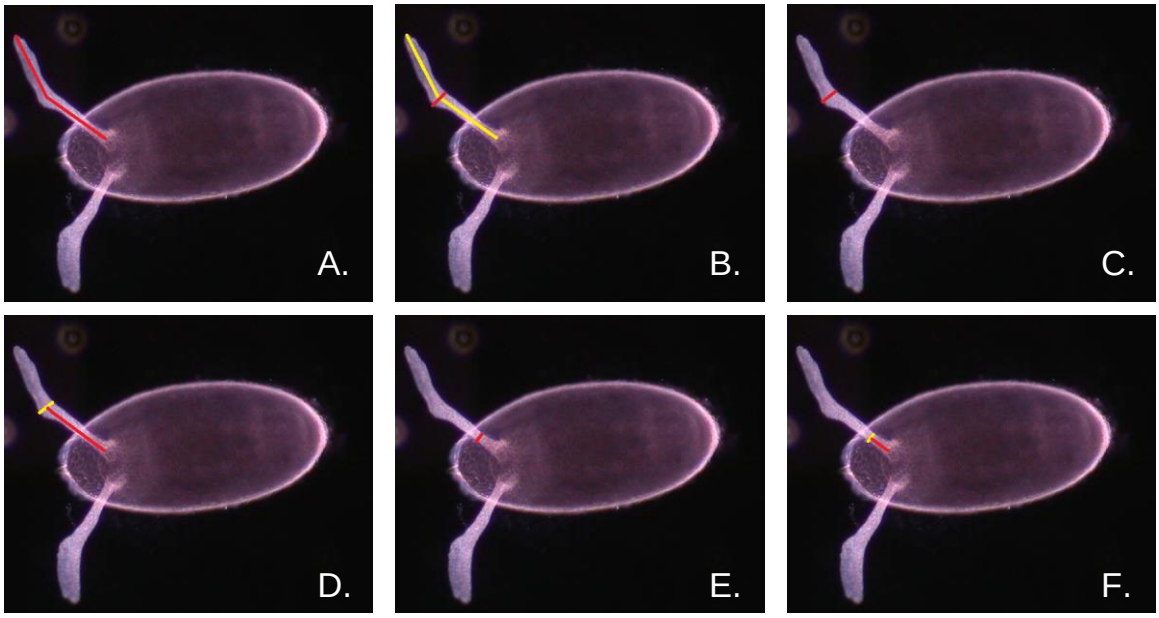

Figure 5. Parameters used to characterize DAs. The lines indicate the way I measured each parameter. Red is the primary measurement. A. Length of appendage. B. Width at a point halfway up the appendage; yellow line is length. C. Maximum width. D. Length to maximum width; yellow line is maximum width. E. Minimum width. F. Length to minimum width; yellow line is minimum width.

well as the halfway width, helped quantify the shape of the appendage – whether it was narrow at the top or bottom.

From these measurements, I calculated several other parameters designed to quantify the shape of the appendage: the percentage length along the appendage of the point of maximum width and minimum width, the range of widths, and the normalized width. Importantly, these percentages gave shape information that was not dependent on size; a large appendage might have a point of maximum width longer than a small appendage simply because the overall DA was longer, but the percentage of the length that the point of maximum width was situated would be the same for two similarly-shaped appendages, regardless of appendage size. The normalized width, obtained by

dividing the maximum width by the length, provided a ratio that could show differences in the shape or flaring of the appendage regardless of size.

In the subset of appendages I measured, the wild type significantly differed from the experimental samples in only three parameters: overall length, maximum width, and normalized width (ANOVA, P= 0.04 between *bunched-lacZ* and *Wnt2*-RNAi). The overall length and maximum width measured the overall size of the appendage, while the normalized width quantified shape, irrespective of appendage size. I subsequently used these parameters, along with the presence or absence of bifurcation, to evaluate each DA I observed (n= 2878).

Wnt2 knock down in the SCs caused a variable aberrant DA phenotype

To reduce expression of the known *Drosophila* Wnt, Hedgehog (HH), Netrin, Semaphorin, and Ephrin proteins, I used a SC *GAL4* driver to express hairpin RNA constructs for each individual signaling protein (Table 1). As negative controls in the first experiment, I used flies that were w^{1118}, *bunched-lacZ*, or the *PG150-GAL4* driver line alone. The previously successful *Notch* gain-of-function line (NGoF) crossed to the *PG150-GAL4* driver line (Fig. 9; Hassigner and Berg, unpublished data) was intended to be the positive control for the experiment, but the cross failed to produce progeny of the critical genotype, likely because the temperature at which the flies were raised inactivated the temperature-sensitive Gal80p and therefore allowed expression of the NGoF in many areas of the developing fly, leading to death. In the second cross, I used w^{1118} and *bunched-lacZ* flies crossed to the *PG150-GAL4* driver as negative controls, and again attempted to use the NGoF crossed to *PG150-GAL4* as a positive control. In this experiment, the NGoF cross failed to produce any progeny, possibly because the NGoF

Table 2. Results from the first RNAi experiment.

Construct	Mean length	P-value	Mean width	P-Value	Mean norm. width	P-value	# of DAs
Controls:							
w1118 only	395.42	N/A	32.75	N/A	0.11	N/A	20
bunched-lacZ	289.53	N/A	37.39	N/A	0.13	N/A	20
PG150-GAL4/FM6, Bar	341.10	**<0.01 (bunched-LacZ), <0.01 (w1118)**	42.78	0.64 (bunched-lacZ), **0.01 (w1118)**	0.13	1.00 (bunched-lacZ), 0.32 (w1118)	20

Driven by PG150-GAL4:		**P-value w1118**	**P-Value bunched-lacZ**		**P-value w1118**	**P-Value bunched-lacZ**		**P-value w1118**	**P-Value bunched-lacZ**	
>UAS-Hh RNAi (43255)	289.95	0.48	1.00	35.13	0.98	1.00	0.12	0.72	1.00	20
>UAS-Wg RNAi	262.64	**<0.01**	0.09	40.16	0.08	0.99	0.16	**0.01**	0.62	20
>UAS-Wnt2 RNAi	262.24	**<0.01**	**0.04**	48.69	**<0.01**	**0.02**	0.19	**<0.01**	**<0.01**	20
>UAS-Ephrin RNAi	293.30	0.52	1.00	36.4	0.91	1.00	0.13	0.68	1.00	20
>UAS-NetrinA RNAi	285.10	0.09	1.00	36.05	0.87	1.00	0.13	0.20	1.00	20
>UAS-Sema1a RNAi	281.80	**0.05**	1.00	35.65	0.92	1.00	0.14	0.30	1.00	20
>UAS-Sema2b RNAi (101842)	279.46	0.23	1.00	46.69	**0.02**	0.38	0.17	**0.03**	0.42	20

Table 3. Results from the second RNAi experiment.

Construct	Mean length	P-value		Mean width	P-Value		Mean norm. width	P-value		# of DAs
Controls:										
w1118, PG150-GAL4	311.58		N/A	36.88		N/A	0.12		N/A	88
bunched lacZ, PG150-GAL4	285.00		N/A	37.12		N/A	0.13		N/A	137
Driven by PG150-GAL4:		**P-value w1118**	**P-Value bunched-lacZ**		**P-value w1118**	**P-Value bunched-lacZ**		**P-value w1118**	**P-Value bunched-lacZ**	
>UAS-Hh RNAi (1402)	287.22	**<0.01**	1.00	38.76	0.79	0.92	0.14	**0.01**	1.00	94
>UAS-Hh RNAi (109454)	287.38	**<0.01**	1.00	36.00	1.00	1.00	0.13	0.73	1.00	128
>UAS-Wg RNAi	276.04	**<0.01**	0.09	35.83	1.00	1.00	0.13	0.34	1.00	70
>UAS-Wnt2 RNAi	289.00	**<0.01**	0.98	36.77	1.00	1.00	0.13	0.51	1.00	112
>UAS-Wnt3/5 RNAi	283.35	**<0.01**	1.00	36.38	1.00	1.00	0.13	0.59	1.00	43
>UAS-Wnt4 RNAi	291.24	**<0.01**	0.84	34.76	0.99	0.66	0.12	1.00	0.41	99
>UAS-Wnt6 RNAi	286.31	**<0.01**	1.00	36.07	1.00	1.00	0.13	0.79	1.00	101
>UAS-Wnt10 RNAi	283.02	**<0.01**	1.00	36.65	1.00	1.00	0.13	0.44	1.00	61
>UAS-WntD RNAi	292.66	**<0.01**	0.35	38.33	0.93	0.99	0.13	0.09	1.00	94
>UAS-Ephrin RNAi	298.08	**<0.01**	**<0.01**	34.65	0.98	0.60	0.12	1.00	**0.02**	89
>UAS-NetrinA RNAi	282.27	**<0.01**	1.00	41.63	0.46	0.58	0.15	**0.03**	0.61	22
>UAS-Sema1a RNAi	275.53	**<0.01**	**0.04**	37.33	1.00	1.00	0.14	**0.01**	0.99	127
>UAS-Sema2b RNAi (108030)	263.49	**<0.01**	**<0.01**	40.51	0.44	0.59	0.15	**<0.01**	**0.02**	36
>UAS-Sema2b RNAi (101842)	287.55	**<0.01**	1.00	34.11	0.75	0.13	0.12	1.00	0.12	93

Table 4. Results from the third RNAi experiment.

Construct	Parents' temp. of raising	Mean length	P-value		Mean width	P-Value		Mean norm. width	P-value		# of DAs
Controls:											
w1118, PG150-GAL4	21° C	288.98		N/A	35.34		N/A	0.12		N/A	144
w1118, PG150-GAL4	25° C	292.74	P=0.91 (w1118, 21° C)		32.57	0.81 (w1118, 21° C)		0.11	P=0.70 (w1118, 21° C)		131
Driven by PG150-GAL4:			**P-value w1118**	**P-value UAS-GFP**		**P-value w1118**	**P-value UAS-GFP**		**P-value w1118**	**P-value UAS-GFP**	
>UAS-GFP	21° C	291.20	N/A	N/A	32.85	N/A	N/A	0.11	N/A	N/A	50
>UAS-NGoF	21° C	167.08	**<0.01**	**<0.01**	63.51	**<0.01**	**<0.01**	0.43	**<0.01**	**<0.01**	35
>UAS-CG9523 RNAi	21° C	269.67	**<0.01 (21° C), <0.01 (25° C)**	**<0.01**	38.68	0.69 (21° C), **<0.01 (25° C)**	**<0.01**	0.15	0.15 (21° C), **<0.01 (25° C)**	**<0.01**	175
>UAS-CG9523 RNAi	25° C	272.23	**<0.01 (21° C), <0.01 (25° C)**	**<0.01**	40.96	**0.03 (21° C), <0.01 (25° C)**	**<0.01**	0.15	**<0.01 (21° C), <0.01 (25° C)**	**<0.01**	156
>UAS-Hh RNAi (1402)	25° C	297.68	**0.05**	0.75	35.71	0.61	0.12	0.12	1.00	0.64	137
>UAS-Wnt2 RNAi	21° C	285.31	1.00 (21° C), 0.95 (25° C)	1.00	33.49	1.00 (21° C), 1.00 (25° C)	1.00	0.12	1.00 (21° C), 0.96 (25° C)	1.00	38
>UAS-Wnt2 RNAi	25° C	283.44	0.36 (21° C), **0.01 (25° C)**	0.72	34.15	0.69 (21° C), 0.98 (25° C)	1.00	0.12	1.00 (21° C), 0.09 (25° C)	0.83	154
>UAS-Sema2b RNAi (101842)	21° C	276.51	**<0.01 (21° C), <0.01 (25° C)**	**0.04**	35.40	1.00 (21° C), 0.08 (25° C)	0.55	0.13	1.00 (21° C), **<0.01 (25° C)**	0.19	117
>UAS-Sema2b RNAi (101842)	25° C	285.46	0.95 (21° C), **0.05 (25° C)**	0.95	35.62	1.00 (21° C), **0.01 (25° C)**	0.30	0.13	1.00 (21° C), **<0.01 (25° C)**	0.06	167

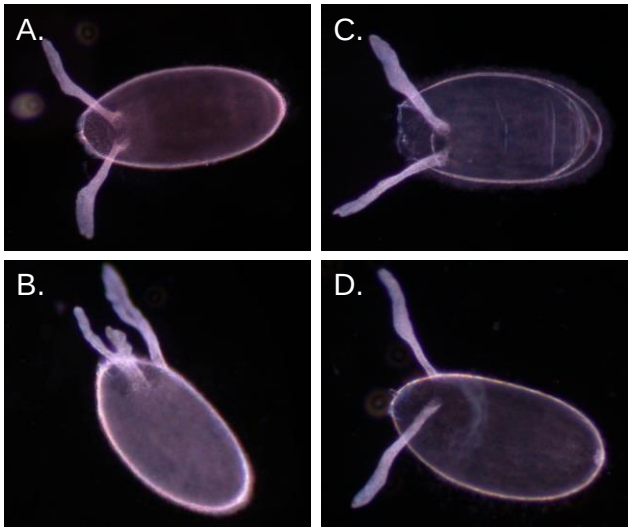

Figure 6. Phenotypes of eggs laid by females expressing wnt2 RNAi. Micrographs showing dorsal (A, C) or dorsolateral (B,D) views of representative eggs. A. Wild-type egg. B. *Wnt2*-RNAi egg, from the first set of experiments. Note the bifurcation of the lower appendage. C. *Wnt2*-RNAi egg from the second set of experiments. D. *Wnt2*-RNAi egg from the third set of experiments. Note in C and D the straight, clean stalks and paddles, without bifurcation.

flies were crossed to *PG150- GAL4* flies that were homozygous for the temperature sensitive *gal80*. I initially set up a mix of vials in which some crosses used *PG150-GAL4* females that were temperature-sensitive *gal80*/CyO and females that were homozygous for temperature-sensitive *gal80*; when the females in these vials laid eggs, I observed that flies homozygous for the *gal80[ts]* chromosome laid very few eggs and subsequently had few progeny. It is possible that there was a background mutation on the temperature-sensitive-*gal80* chromosome that reduced fertility when homozygous, allowing those with a *CyO* chromosome to be more fertile. In the third experiment, I used w^{1118} and *UAS-GFP*^{S65T} (enhanced GFP) crossed to *PG150-GAL4* as negative controls, and *UAS-opa1*-RNAi, *UAS-CG9523*-RNAi, and *UAS*-NGoF crossed to *PG150-GAL4* as positive controls; the *opa1*-RNAi cross produced few progeny, but the other two crosses yielded females that laid a sufficient number of eggs to use as a positive control. Previous unpublished work by Ariel Altaras and Robert Matlock in our lab had shown that stretch-cell-specific RNAi of *opa1* or *CG9523* produced consistent and highly penetrant DA defects.

In the initial experiment, I detected no significant differences in DA morphology except in eggs produced by females expressing RNAi for *Wnt2*. These eggs had a clear morphological defect, with 28% (39/140) of appendages branching during their formation, producing a 'tuning fork' effect (Fig. 6). Intriguingly, knockdown of *Semaphorin-2b* also produced a similar phenotype, although the effect was less penetrant, exhibited by 10% of the appendages (14/135). In a second RNAi experiment, however, where the larvae were raised at 21° C instead of at 25° C (to avoid death of the positive control flies), I did not observe major DA defects in either the *Semaphorin*-RNAi or the *Wnt2*-RNAi eggs. The grossly normal phenotype was true for both gross morphology and lengths of appendages in the *Wnt2*-RNAi eggs (ANOVA, P=0.98). Unfortunately, the flies intended to be a positive control in the second experiment were few and laid few eggs, rendering the results difficult to interpret.

In the third experiment, I limited my experimental analyses to three samples, *Wnt2* (V-104338), *hh* (V-1402), and *Sema-2b* (V-101842), but raised one set of the progeny at 25° C and another set of the progeny at 21° C. Regardless of temperature, I observed no gross physical differences between the *Wnt2*-RNAi eggs and the negative control w^{1118} and *UAS-GFP* eggs, and only the *Sema-2b*-RNAi had any significant differences in eggs from flies raised at 21° C and 25° C (Table 5). The *Wnt2*-RNAi eggs from parents raised at 25° C were significantly shorter than the w^{1118} raised at 25° C ($P<0.01$), but not the *UAS-GFP* eggs (P=0.72). Note, however, that the mean length of the dorsal appendages on the *UAS-GFP* eggs was similar to that of the w^{1118} control; since I measured fewer *UAS-GFP* samples, however, the difference in length with the *Wnt2*-RNAi dorsal appendages did not meet the standards for statistical significance.

Table 5. Differences in eggs based on parent's temperature of raising.

Construct	Parents' temp. of raising	Mean length	P-value to 21° C	Mean width	P-value to 21° C	Mean norm. width	P-value to 21° C	# of DAs
w1118, PG150-GAL4	21° C	288.98	N/A	35.34	N/A	0.12	N/A	144
w1118, PG150-GAL4	25° C	292.74	0.91	32.57	0.81	0.11	0.70	131
Driven by PG150-GAL4:								
>UAS-CG9523 RNAi	21° C	269.67	N/A	38.68	N/A	0.15	N/A	175
>UAS-CG9523 RNAi	25° C	272.23	0.99	40.96	0.64	0.15	1.00	156
>UAS-Wnt2 RNAi	21° C	285.31	N/A	33.49	N/A	0.12	N/A	38
>UAS-Wnt2 RNAi	25° C	283.44	1.00	34.15	1.00	0.12	1.00	154
>UAS-Sema2b RNAi (101842)	21° C	276.51	N/A	35.40	N/A	0.13	N/A	117
>UAS-Sema2b RNAi (101842)	25° C	285.46	**0.02**	35.62	1.00	0.13	1.00	167

The *Wnt2*-RNAi egss were not significantly different from w^{1118}, *UAS-GFP*, or *hh-RNAi* eggs in width (P=1.00, 0.93, and 0.60, respectively) or shape (P=1, 0.66, and 1, respectively). The *Sema-2b* RNAi did not produce a gross morphological defect (Fig. 7), but did produce appendages at 21° C that were significantly shorter than w^{1118} and *hh-RNAi*, and *UAS-GFP* (P<0.01 for both w^{1118} and *hh-RNAi*, P=0.04 for *UAS-GFP*). In summary, RNAi against *Wnt2* and *Sema-2b* produced shorter dorsal appendages compared to several controls and one other experimental sample, but did not reproduce the bifurcations and other obvious malformations observed in the first experiment.

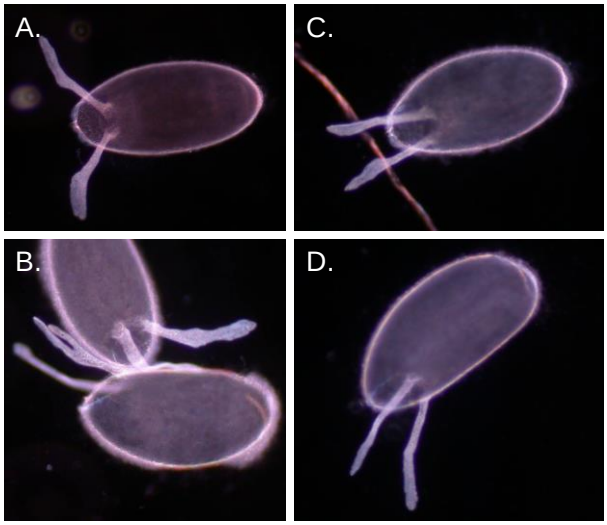

Figure 7. Phenotypes of *Semaphorin-2b*-RNAi. Laid eggs. Anterior is to the left, dorsal is pointing out of the page for A,C, up for B, down for D. A. A representative wild-type egg. B. Representative *Semaphorin-2b*-RNAi eggs, from the first set of experiments. Note the bifurcation of the upper appendage in the lower egg. C. A representative *Semaphorin-2b*-RNAi egg from the second set of experiments. D. A representative *Semaphorin-2b*-RNAi egg from the third set of experiments. Note the lack of bifurcation in C and D.

Cultured egg chambers have variable DA morphology

To determine if the culture system could reliably produce wild-type eggs, I cultured over 300 eggs from two fly strains, w^{1118} and *E(spl)m7-lacZ*. I used this second strain as a reporter of Notch activity (Pines *et al.*, 2010). Neither strain had known DA defects in laid eggs. When culturing the eggs in Robb's medium, it became apparent that the phenotype of the DAs varied widely from egg to egg and trial to trial (Fig. 8). Overall, 26% of wild-type cultured eggs looked normal, 57% looked mildly aberrant, and 17% were severely aberrant (n=137). The initial, pre-measured level of variability was sufficiently low, however, that I predicted that reproducible differences in morphology due to experimental addition of molecules would be noticeable, so I continued with this line of experimentation.

Treatment with Jagged peptide had no effect on DA morphology

Previous work in the Berg lab had shown that the hyperactivation of Notch specifically in the SCs caused a severe DA defect (Fig. 9, Hassinger and Berg,

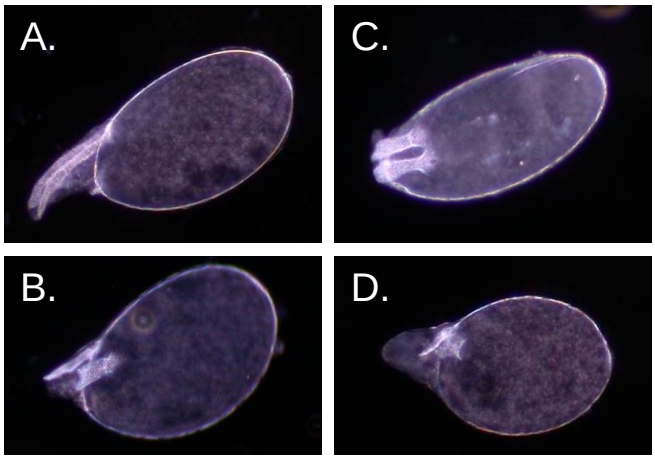

Figure 8. Cultured egg chambers display highly variable phenotypes. Representative dark field micrographs of cultured egg chambers. Anterior is to the left, dorsal is up in A, B, and D, and pointing out of the page in C. A. – D. I cultured these four egg chambers of the *E(spl)m7-lacZ* genotype in the same batch, without any substances added to the Robb's medium, and yet these eggs display highly variable DA morphology.

unpublished data). I therefore used activation of the Notch pathway as a positive control for the culture assay. Furthermore, soluble Jagged peptide activates the Notch pathway in various cell culture systems (Nickoloff *et al.*, 2002), so I chose it to be the ligand for the cell culture assay. As its potency in an egg culture assay was unknown, I used several concentrations between 40 µM and 200 µM Jagged to test its efficacy. Higher

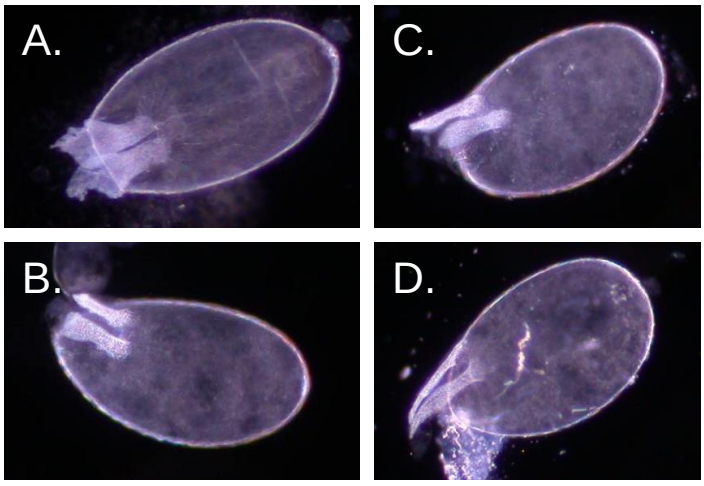

Figure 9. Addition of Jagged does not recapitulate the NGoF phenotype. Anterior is to the left, dorsal is pointing out of the page for A and up for B, C, and D. A. The NGoF phenotype includes short, wide stalks and wide, feathery paddles, as shown by this egg laid by a female of the *PG150-GAL4>UAS-NGoF* genotype. B, C, and D are of the *E(spl)m7-lacZ* genotype, used as a reporter of Notch function while culturing egg chambers. B. An egg chamber cultured in Robb's medium with no additives. C. An egg chamber cultured in Robb's medium with 100 µM Jagged. D. An egg chamber cultured in Robb's medium with 200 µM Jagged. Note the similarity between the three cultured egg chambers and the narrowness and smoothness of these appendages compared to the appendages of the *PG150-GAL4>UAS-NGoF* egg.

concentrations were not feasible due to limits of solubility and limits to the starting peptide concentrations available to us. None of the concentrations of Jagged produced a significant difference in length or maximum width of appendages (Table 6, Fig. 9). Furthermore, the negative controls produced severe defects in appendage morphology at approximately the same rate as the treatment, suggesting that the Jagged treatment in cultured egg chambers did not replicate the phenotype seen in earlier genetic experiments.

To test if Jagged activated the Notch pathway in the culture assay, I analyzed the expression of the *E(spl)m7-lacZ* reporter using a β-galatactosidase staining assay (n=83) and *bunched-lacZ* as a positive control (n=53). I found that *E(spl)m7-lacZ* cultured without treatment displayed strong staining in the border cells; this expression persisted until the follicle cells deteriorated and fell off the egg. Furthermore, some staining occurred around the DA-forming cells and the cells that form the operculum. Addition of Jagged to the culture medium weakly increased staining in the main-body columnar follicle cells, but had little if any effect on the strength of staining on the stretch cells or in areas that normally stained.

Table 6. Results from cultured egg chambers.

Treatment	Mean length	P-value	Mean width	P-value	Mean norm. width	P-value	# of DAs
0 µM Jagged	114.48	N/A	32.36	N/A	0.33	N/A	85
100 µM Jagged	104.88	0.18	31.36	0.06	0.37	0.91	70
125 µM Jagged	125.57	0.66	38.69	0.53	0.35	0.97	35
200 µM Jagged	101.75	0.47	30.12	0.19	0.43	0.70	26
untreated	120.94	N/A	32.83	N/A	0.31	N/A	55
0 µM IWR-1	120.70	0.90	33.67	0.81	0.34	0.40	76
10 µM IWR-1	84.51	**<0.01**	26.36	**0.02**	0.39	0.25	49

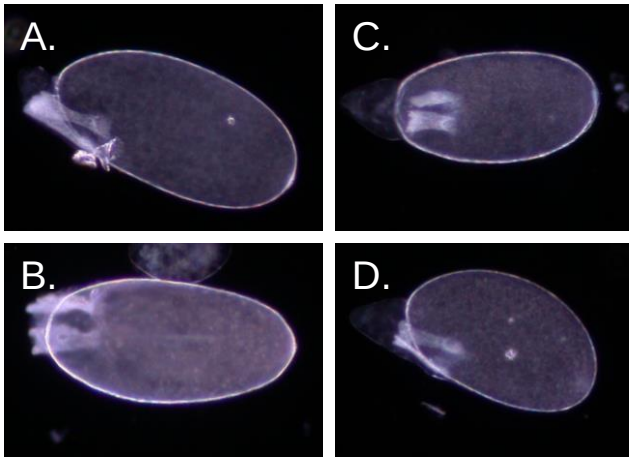

Figure 10. Addition of IWR-1 produces a slight shortening of the appendages. Anterior is to the left; dorsal is down in A and D and facing out of the page in B and C. All egg chambers are of the w^{1118} genotype. A. Egg chamber cultured in Robb's medium with no additives. B. Egg chamber cultured in Robb's medium with DMSO. C, D. Egg chambers cultured in Robb's medium with 10 µM IWR-1. Such eggs often have shorter or thinner appendages than their DMSO-treated or untreated counterparts (see Table 6).

Adding the Wnt-blocker IWR-1 shortened appendages

I also conducted tests with the Wnt-blocker IWR-1, which strongly and selectively inhibits Wnt response at low concentrations in mouse cells, human colon cancer cells, and adult zebrafish (Chen *et al.*, 2009). To test if IWR-1 addition would elicit an aberrant DA phenotype in my culture system, I added 10 µM IWR-1 in DMSO and compared egg phenotype to that produced by the addition of DMSO alone. Although the appendages had variable phenotypes in the set of treated eggs, including occasionally becoming very narrow (Fig. 10), they were significantly shorter than both untreated and DMSO-treated appendages (Table 6) (ANOVA, Gaines-Howell, $P<0.01$ for untreated and for DMSO).

Discussion

Discovering the guidance signals responsible for guiding the DAs would greatly enhance our knowledge of the guidance of already formed tubes. From the research that I

have done thus far, there are hints about what the DA guidance signal might be, but the story is far from definitive. Both the culture system and the RNAi indicate that Wnts could play a role in the guidance of the DAs, but neither approach has yet produced conclusive results. Both techniques have encountered problems that make the analysis of the current data less than satisfactory.

The culture system is too variable to assay drugs that modify signaling-pathways

The culture system faces the obstacle of reproducibility. Although it is in theory a powerful tool, the highly variable DA morphology obtained even among the supposed negative controls highlights a problem with the approach. It is quite possible that a signal may be required for proper chorion secretion or cross-linking that is not produced by the egg chamber itself, yet is rather produced by the surrounding ovarian tissue. In addition, there could be day-to-day variations in technique, contaminants in the medium, age of the 24-well plate, or other variables between experiments that affect the morphology of the DAs yet are unrelated to the choice of medium. Until the source of the variability can be found and prevented, the culture system can produce hints to guide further research – such as the reaction to inhibition of Wnts – but not conclusive, publishable evidence, as there is no solid control yet to ensure the veracity of the findings.

To make the culture system more reproducible, I would first compare the differences, if any, between my completely freshly made Robb's medium and Schneider's medium. Previous work (Dorman *et al.*, 2004) identified no significant difference between Robb's and Schneider's media, but the quantification involved analysis of nurse-cell dumping under a dissecting microscope and tube elongation by

confocal analysis, rather than exact measurements of DA length and width. If there were a difference, it would suggest that Schneider's medium contained a factor essential to proper growth. I could then attempt to elucidate this factor by adding various compounds, both potential signals and simple organic molecules such as cholesterol, to the medium and determining whether any affected DA formation. If these methods did not work, I could use mass spectrometry to discover what molecules differed in amount between Schneider's and Robb's, and test those. Alternatively, I could use a different method of evaluation, possibly by looking at the real-time movements of DA-forming cells using confocal microscopy; this approach would be more time consuming but it could distinguish a defect in chorion secretion or cross-linking from a true DA-tube formation defect.

Notch gain of function could be a positive control for the culture system

Although Jagged produced significant defects in DA morphology, the phenotype did not resemble that of the stretch-cell-specific N-GoF. Notch is a membrane-bound protein, and thus it signals in an extremely restricted domain, requiring direct cell-to-cell contact to initiate signaling. In the culture system, I used a soluble protein to activate Notch; this approach would activate Notch in an extended domain – not only in the SCs, but also in the columnar follicle cells, including the DA-forming cells. This difference could have caused the difference in phenotype between the highly protrusive defect seen in *PG150-GAL4>UAS-NGoF* eggs and the simple DA shortening seen in those cases where addition of Jagged seemed to produce a defect (Fig. 9). It is also possible that

slight activation of Notch signaling in the columnar follicle cells contributed to the somewhat round appearance of these cultured egg chambers.

A better positive control would be to culture the *PG150-GAL4>UAS-NGoF* egg chambers, both alone and with DAPT, an inhibitor of Notch cleavage and thus Notch signaling. The gain of function construct I used allows constitutive cleavage of the transcription factor domain of Notch, which then translocates to the nucleus; DAPT would block this cleavage, preventing the over-activation of Notch signaling. I did not use this approach initially due to the difficulty of obtaining *PG150-GAL4>UAS-NGoF* females; these females must be raised at a low temperature to prevent death from aberrant expression of the over-activated Notch, and even with such precautions, they do not appear in Mendelian ratios. Further use of the culture system requires verification of its efficacy, and thus would warrant such efforts.

RNAi suggests a role for WNT signaling in DA formation

The RNAi experiments also suggested a role for Wnts in DA guidance. In the first RNAi experiment, RNAi against *Wnt2* had a profound effect on DA formation. This result, however, was not repeated in further trials. It is possible that the *P* element containing the RNAi was lost between the first and second experiments, as the *Wnt2*-RNAi stock experienced a crash down to a pair of males, which I then crossed to virgin females from a balancer line. Maintenance of the eye color marker, however, renders this possibility unlikely, unless the stock was in some way contaminated. The *PG150-GAL4* driver clearly works, as the positive controls demonstrated significantly shorter DAs (Table 4). The temperature at which I raised the flies did not have an effect on the DA

morphology except in the case of *Sema-2b* RNAi on DA length (Table 5), although the mating temperature differed in the second and third experiments from the first experiment. I monitored the temperature in the incubator during the third experiment, and the temperature remained steady at 30° C. It is possible that during the initial experiment, there was a spike in the temperature of the incubator, causing an increase in the general severity of phenotypes displayed – especially the increased bifurcation noted in both the *Wnt2* and *Sema2b* RNAi eggs. I could test this possibility by deliberately increasing the temperature of the incubator and seeing if the eggs laid by *Wnt2*-RNAi and *Sema2b*-RNAi flies resembled those from the first trial. Until such experiments are performed, however, it remains unclear why the initial result was not repeated.

To ascertain whether WNT-2 functions in DA-tube guidance, I could analyze eggs produced by females homozygous for the *Wnt2* null mutation $Wnt2^{O}$, which is caused by a stop codon at the fortieth amino acid of the protein (Kozopas *et al.*, 1998). The allele is male sterile, but not female sterile, allowing easy analysis of eggs laid by *Wnt2*-null females. If these eggs displayed DA defects, it would be compelling evidence that *Wnt2* is required for proper DA formation. If they do not display defects, it does not indicate that *Wnt2* is not necessary; rather, it is possible that the *Wnt2*-RNAi has an off-target effect on one or more genes in the Wnt pathway, or multiple Wnts are actually required for proper DA formation. To test this hypothesis, I could use RNAi against different Wnts in the *Wnt2*-null background and examine the DAs of the laid eggs to see if any increased the potential effect of the *Wnt2* null.

Semaphorin-2b might contribute to DA guidance

Although the striking result of DA bifurcation did not repeat for the *Semaphorin-2b* RNAi, this reduction of function produced significant differences from the wild type in each experiment. In the first experiment, *Sema-2b*-RNAi eggs displayed a partially penetrant but severe DA bifurcation defect (Fig. 7). In the second test, a different RNAi construct against *Semaphorin-2b* resulted in significantly shorter DAs compared to both controls ($P<0.01$). In the third, the original RNAi construct, which was the only *Sema-2b* construct used in this experiment, also demonstrated significantly shorter appendages when raised at 21° C compared to eggs produced by the w^{1118} crossed to *PG150-GAL4* control and the *UAS-GFP* control ($P<0.01$ and $P=0.04$, respectively). These results, taken together, suggest that Semaphorin-2b might play a role in signaling, but it is doubtful that it comprises the entire signal, given the modest nature of the observed effects. Development of null alleles and study of their eggs, if possible, might be a fruitful line of inquiry. Alternatively, I could use a driver that is expressed earlier during egg chamber development, as the protein might be manufactured before the *PG150-GAL4* driver activates at Stage 10 of egg development; Semaphorin-2b is probably a relatively stable protein as it is required for long-term neuronal guidance (Wu *et al.*, 2011), and RNAi cannot remove protein that has already been made.

Analysis of the advantages and uses of the methods I used

The methods I used each have distinct advantages. The culture system is a promising tool, if the flaws with reproducibility can be eliminated. Using the culture system, one can have precise temporal control over disruption or activation of signals, and small molecule agonists and antagonists have immediate effect, not dependent on the

degradation of already-made protein. Moreover, the agonists and antagonists can often block or stimulate a whole pathway at once, or even several different pathways simultaneously, circumventing problems with redundant genes or parallel pathways and allowing faster screening that could be dissected subsequently through genetic means. Until it is easily reproducible, however, the culture system cannot be considered a reliable tool.

The use of RNAi also has certain advantages. It has strict spatial control, as long as appropriate drivers are available, and thus can ensure that the eggs are not malformed due to a defect in the main-body columnar cells or simply because the adult fly is sickly due to some defect unrelated to egg development. Although off-target effects can be frustrating and difficult to analyze, they can occasionally assist in discovering a phenotype by knocking down more than one gene in a pathway, or knocking down two closely related and partially redundant pathways to make an otherwise obscure phenotype clear. It cannot completely remove expression of a given gene, nor can it clear protein that was formed before its activation, but its ability to knock down essential genes makes it an invaluable tool in determining the signals that help to form the DAs.

Despite the technical challenges encountered in this project, there have been clear and interesting results. I discovered that *Semaphorin-2b* plays a role in the guidance of the DAs, which has never before been reported. Furthermore, I found hints that *Wnt2* in particular, or the Wnts in general, play a role in guiding the DAs. These observations suggest that both soluble and membrane-bound signals may play a role in guiding tubes. With follow-up on some of the intriguing results presented here, much more could be

learned about the signals that guide tubes, and subsequently, the mechanisms by which signals guide tubes.

Literature Cited:

Boyle, M.J. and Berg, C.A. (2009). Control in time and space: Tramtrack69 cooperates with Notch and Ecdysone to repress ectopic fate and shape changes during *Drosophila* egg chamber maturation. Development. *136*:4187-4197.

Boyle, M.J., French, R.L., Cosand, K.A., Dorman, J.B., Kiehart, D.P., and Berg, C.A. (2010). Division of labor: subsets of dorsal-appendage-forming cells control the shape of the entire tube. Dev Biol. *346*:68-79.

Castets, M. and Mehlen, P. (2010). Netrin-1 role in angiogenesis: to be or not to be a pro-angiogenic factor? Cell Cycle. *9*:1466-1471.

Chen, B., Dodge, M.E., Tang, W., Lu, J., Ma, Z., Fan, C.W., Wei, S., Hao, W., Kilgore, J., Williams, N.S., Roth, M.G., Amatruda, J.F., Chen, C., and Lum, L. (2009). Small molecule-mediated disruption of Wnt-dependent signaling in tissue regeneration and cancer. Nat Chem Biol. *5*:100-107.

Davidson, L.A. and Keller, R.E. (1999). Neural tube closure in *Xenopus laevis* involves medial migration, directed protrusive activity, cell intercalation and convergent extension. Development. *126*:4547-4556.

Dorman, J.B., James, K.E., Fraser, S.E., Kiehart, D.P., and Berg, C.A. (2004). *bullwinkle* is required for epithelial morphogenesis during *Drosophila* oogenesis. Dev Biol. *267*:320-341.

Fenstermaker, A.G., Prasad, A.A., Bechara, A., Adolfs, Y., Tissir, F., Goffinet, A., Zou, Y., and Pasterkamp, R.J. (2010). Wnt/planar cell polarity signaling controls the anterior-posterior organization of monoaminergic axons in the brainstem. J Neurosci. *30*:16053-16064.

Groenman, F., Unger, S., and Post, M. (2005). The molecular basis for abnormal human lung development. Biol Neonate. *87*:164-177.

Hinton H.E. (1969). Respiratory systems of insect egg shells. Annu Rev Entomol. *14*:343-368.

Hogan, B.L. and Kolodziej, P.A. (2002). Organogenesis: molecular mechanisms of tubulogenesis. Nat Rev Genet. *3*:513-523.

Horne-Badovinac, S., Lin, D., Waldron, S., Schwarz, M., Mbamalu, G., Pawson, T., Jan, Y., Stainier, D.Y., and Abdelilah-Seyfried, S. (2001). Positional cloning of *heart and soul* reveals multiple roles for PKC lambda in zebrafish organogenesis. Curr. Biol. *11*:1492–1502.

Jordan, K.C., Hatfield, S.D., Tworoger, M., Ward, E.J., Fischer, K.A., Bowers, S., and Ruohola-Baker, H. (2005). Genome wide analysis of transcript levels after perturbation of the EGFR pathway in the *Drosophila* ovary. Dev Dyn. *232*:709-724.

Kar, S., Deb, M., Sengupta, D., Shilpi, A., Bhutia, S.K., and Patra, S.K. (2012). Intricacies of hedgehog signaling pathways: a perspective in tumorigenesis. Exp Cell Res. *318*:1959-1972.

Kozopas, K.M., Samos, C.H., and Nusse, R. (1998). DWnt-2, a *Drosophila* Wnt gene required for the development of the male reproductive tract, specifies a sexually dimorphic cell fate. Genes Dev. *12*:1155-1165.

Lubarsky, B. and Krasnow, M.A. (2003). Tube morphogenesis: making and shaping biological tubes. Cell. *112*:19-28.

Maung, S.M. and Jenny, A. (2011). Planar cell polarity in *Drosophila*. Organogenesis. *7*:165-179.

Neufeld, G., Sabag, A.D., Rabinovicz, N., and Kessler, O. (2012). Semaphorins in Angiogenesis and Tumor Progression. Cold Spring Harb Perspect Med. *2*: a006718.

Nickoloff, B.J., Qin, J.Z., Chaturvedi, V., Denning, M.F., Bonish, B., and Miele, L. (2002). Jagged-1 mediated activation of notch signaling induces complete maturation of human keratinocytes through NF-kappaB and PPARgamma. Cell Death Differ. *9*:842-855.

Niehrs, C. (2012). The complex world of WNT receptor signalling. Nat Rev Mol Cell Biol. *13*:767-779.

Peri, F. and Roth, S. (2000). Combined activities of *Gurken* and *decapentaplegic* specify dorsal chorion structures of the *Drosophila* egg. Development. *127*:841-850.

Pines, M.K., Housden, B.E., Bernard, F., Bray, S.J., and Röper, K. (2010). The cytolinker Pigs is a direct target and a negative regulator of Notch signalling. Development *137*: 913-922.

Proffitt, K.D. and Virshup, D.M. (2012). Precise regulation of porcupine activity is required for physiological Wnt signaling. J Biol Chem. *287*:34167-34178.

Rittenhouse, K.R. and Berg, C.A. (1995). Mutations in the *Drosophila* gene *bullwinkle* cause the formation of abnormal eggshell structures and bicaudal embryos. Development. *121*:3023-3033.

Robb, J.A. (1969). Maintenance of imaginal discs of *Drosophila melanogaster* in chemically defined media. J Cell Biol. *41*:876-885.

Salvucci, O. and Tosato, G. (2012). Essential roles of EphB receptors and EphrinB ligands in endothelial cell function and angiogenesis. Adv Cancer Res. *114*:21-57.

Schoenwolf, G.C. and Powers, M.L. (1987). Shaping of the chick neuroepithelium during primary and secondary neurulation: Roll of cell elongation. Anatomical Record. *218*:182–195.

Serafini, T., Kennedy, T.E., Galko, M.J., Mirzayan, C., Jessell, T.M., and Tessier-Lavigne, M. (1994). The netrins define a family of axon outgrowth-promoting proteins homologous to *C. elegans* UNC-6. Cell. *78*:409-424.

Simon, J.A., Sutton, C.A., Lobell, R.B., Glaser, R.L., and Lis, J.T. (1985). Determinants of heat shock-induced chromosome puffing. Cell. *40*:805-817.

Streit, A., Berliner, A.J., Papanayotou, C., Sirulnik, A., and Stern, C.D. (2000). Initiation of neural induction by FGF signalling before gastrulation. Nature. *406*:74-78.

Tran, D.H. and Berg, C.A. (2003). *bullwinkle* and *shark* regulate dorsal-appendage morphogenesis in *Drosophila* oogenesis. Development. *130*:6273-6282.

Tran, T.S., Kolodkin, A.L., and Bharadwaj, R. (2007). Semaphorin regulation of cellular morphology. Annu Rev Cell Dev Biol. *23*:263-292.

Villar-Cerviño, V., Molano-Mazón, M., Catchpole, T., Valdeolmillos, M., Henkemeyer, M., Martínez, L.M., Borrell, V., and Marín, O. (2013). Contact repulsion controls the dispersion and final distribution of cajal-retzius cells. Neuron. *77*:457-471.

Ward, E.J. and Berg, C.A. (2005). Juxtaposition between two cell types is necessary for dorsal appendage tube formation. Mech Dev. *122*:241-255.

Ward, E.J., Zhou, X., Riddiford, L.M., Berg, C.A., and Ruohola-Baker, H. (2006). Border of Notch activity establishes a boundary between the two dorsal appendage tube cell types. Dev Biol. *297*:461-470.

Wieschaus, E. and Nüsslein-Volhard, C. (1986). Looking at embryos. In *Drosophila*: a Practical Approach (ed. D. B. Roberts), pp. 199-227. Oxford: IRL Press.

Wu, Z., Sweeney, L.B., Ayoob, J.C., Chak, K., Andreone, B.J., Ohyama, T., Kerr, R., Luo, L., Zlatic, M., and Kolodkin A.L. (2011). A combinatorial semaphorin code instructs the initial steps of sensory circuit assembly in the *Drosophila* CNS. Neuron. *70*:281-298.

Appendix A: Composition of Robb's Medium (from Robb, 1969)

Stock solution	Compound	Concentration in R-14
		moles/liter
No stock*	Cholesterol	Saturated at 23°C
14-1 (10 ×)	L-Alanine	1.6×10^{-4}
	L-Asparagine	2.0×10^{-4}
	L-Aspartic acid	1.6×10^{-4}
	L-Proline	3.2×10^{-4}
	L-Serine	1.6×10^{-4}
	Glycine	1.6×10^{-4}
	β-Alanine	1.0×10^{-4}
14-2 (10 ×)	L-Arginine HCl	2.0×10^{-3}
	L-Glutamine	4.0×10^{-3}
	L-Histidine HCl	4.0×10^{-4}
	L-Isoleucine	6.4×10^{-4}
	L-Leucine	6.4×10^{-4}
	L-Lysine HCl	8.0×10^{-4}
	L-Methionine	2.0×10^{-4}
	L-Phenylalanine	4.0×10^{-4}
	L-Threonine	7.4×10^{-4}
	L-Tryptophan	8.0×10^{-5}
	L-Tyrosine	3.2×10^{-4}
	L-Valine	6.4×10^{-4}
14-3 (10 ×)‡	L-Cystine HCl	2.6×10^{-4}
14-4 (10 ×)	Fumaric acid (Na salt)	1.5×10^{-2}
	α-Ketoglutaric acid (Na salt)	1.9×10^{-2}
	Malic acid	4.3×10^{-2}
	Pyruvic acid (Na salt)	8.0×10^{-4}
	Succinic acid (Na salt)	4.5×10^{-3}
14-5 (0.25 N)§	NaOH	Approx. 2.5×10^{-2}
14-6 (10 ×)	Glucose	1.0×10^{-2}
	Sucrose	8.8×10^{-2}
14-7 (10 ×)	$MgSO_4 \cdot 7H_2O$	1.2×10^{-3}
	$MgCl_2 \cdot 6H_2O$	1.2×10^{-3}
14-8 (10 ×)	$CaCl_2 \cdot 2H_2O$	1.2×10^{-3}
14-9 (10 ×)	NaCl	2.5×10^{-2}
	KCl	3.8×10^{-2}
	Na_2HPO_4	2.0×10^{-3}
	KH_2PO_4	3.7×10^{-4}
14-10 (100 ×)	$FeSO_4 \cdot 7H_2O$	2.4×10^{-6}
14-11 (1000 ×)	$ZnSO_4 \cdot 7H_2O$	2.4×10^{-6}
14-12 (100 ×)	Lipoic acid	8.0×10^{-9}
	Thymidine	2.4×10^{-6}
	$CuSO_4 \cdot 5H_2O$	8.0×10^{-8}
14-13 (100 ×)	Biotin	2.5×10^{-8}
	Choline chloride	1.0×10^{-4}
	Folic acid	2.0×10^{-6}
	myo(i)-Inositol	7.8×10^{-4}
	Nicotinamide	6.6×10^{-6}
	D-Ca Pantothenate	3.3×10^{-6}
	Para-aminobenzoic acid	6.0×10^{-6}
	Pyridoxal HCl	4.6×10^{-6}
	Riboflavin	2.0×10^{-7}
	Thiamine HCl	2.6×10^{-6}
14-14 (100 ×)	Vitamin B_{12}	8.0×10^{-7}
	Putrescine dihydrochloride	8.0×10^{-7}
14-15 (1000 ×)	Phenol red	3.3×10^{-6}
14-16 (100 ×)	Penicillin	100 Units/ml
	Streptomycin	100 μg/ml
14-17 (1000 ×)‖	Linoleic acid	2.4×10^{-7}

* About 2 mg of dry cholesterol were added to mixing vessel.
‡ Discarded if precipitate formed upon thawing.
§ pH adjusted to 7.1 with 0.25 N NaOH.
‖ Prepared fresh each month by using absolute ethanol and added just before use.